Oncogene (2021) 40:2285–2295
https://doi.org/10.1038/s41388-021-01688-7

ARTICLE

Mitochondrial uncoupler MB1-47 is efficacious in treating hepatic metastasis of pancreatic cancer in murine tumor transplantation models

Amer Alasadi[1,2] · Bin Cao[3] · Jingjing Guo[1] · Hanlin Tao[1] · Juan Collantes[1] · Victor Tan[1] · Xiaoyang Su[4] · David Augeri[3] · Shengkan Jin[1]

Received: 27 May 2020 / Revised: 19 January 2021 / Accepted: 27 January 2021 / Published online: 1 March 2021

Abstract

Pancreatic ductal adenocarcinoma (PDA) is aggressive cancer characterized by rapid progression, metastatic recurrence, and highly resistant to treatment. PDA cells exhibit aerobic glycolysis, or the Warburg effect, which reduces the flux of pyruvate into mitochondria. As a result, more glycolytic metabolites are shunted to pathways for the production of building blocks (e.g., ribose) and reducing agents (e.g., NADPH) for biosynthesis that are necessary for cell proliferation. In addition, PDA cells are highly addicted to glutamine for both maintaining biosynthetic pathways and achieving redox balance. Mitochondrial uncoupling facilitates proton influx across the mitochondrial inner membrane without generating ATP, leading to a futile cycle that consumes glucose metabolites and glutamine. We synthesized a new mitochondrial uncoupler MB1-47 and tested its effect on cancer cell metabolism and the anticancer activity in pancreatic cancer cell models and murine tumor transplantation models. MB1-47 uncouples mitochondria in the pancreatic cancer cells, resulting in: (1) the acceleration of pyruvate oxidation and TCA turnover; (2) increases in AMP/ATP and ADP/AMP ratios; and (3) a decrease in the synthesis rate of nucleotides and sugar nucleotides. Moreover, MB1-47 arrests cell cycle at G_0–G_1 phase, reduces clonogenicity, and inhibits cell growth of murine and human pancreatic cancer cells. In vivo studies showed that MB1-47 inhibits tumor growth in murine tumor transplantation models, and inhibits the hepatic metastasis when tumor cells were transplanted intrasplenically. Our results provide proof of concept for a potentially new strategy of treating PDA, and a novel prototype experimental drug for future studies and development.

Introduction

Pancreatic ductal adenocarcinoma (PDA) is an incurable and devastating cancer characterized by rapid progression, metastatic recurrence, and high resistance to treatments [1, 2]. PDA is the fourth leading cause of cancer-related death in the United States with a 5-year survival rate of only 6% and a median survival rate of fewer than 6 months after diagnosis [1, 3]. In many patients, PDA is not diagnosed until it has reached an advanced metastatic stage [4]. Only about 20% of patients are eligible for resection surgery, of which most will eventually have tumor recurrence [5]. Current chemotherapeutic options for patients are not effective [6]. Although the reason why PDA is insensitive to chemotherapeutic agents is not fully understood, it was proposed that the high degree of genetic heterogeneity might be a factor [3, 7–10].

Regardless of the genetic heterogeneity, the PDA cells share a potential therapeutic vulnerability lying in the

These authors contributed equally: Amer Alasadi, Bin Cao

Supplementary information The online version contains supplementary material available at https://doi.org/10.1038/s41388-021-01688-7.

✉ Shengkan Jin
victor.jin@rutgers.edu

[1] Department of Pharmacology, Robert Wood Johnson Medical School, Rutgers, The State University of New Jersey, Piscataway, NJ, USA

[2] Graduate Program of Physiology and Integrative Biology, Robert Wood Johnson Medical School, Rutgers, The State University of New Jersey, Piscataway, NJ, USA

[3] Medicinal Chemistry Department, Ernest Mario School of Pharmacy, Rutgers, The State University of New Jersey, Piscataway, NJ, USA

[4] Department of Medicine, Robert Wood Johnson Medical School, Rutgers, The State University of New Jersey, Piscataway, NJ, USA

reliance on aerobic glycolysis, known as the Warburg effect [11–13]. In the presence of oxygen, the PDA cancer cells convert a majority of pyruvate derived from glycolysis to lactate, in contrast to normal cells in which the majority of the pyruvate enters the mitochondria for oxidative phosphorylation [14, 15]. It is becoming clear that the most important function of the Warburg effect to tumorigenesis is to reduce glycolysis flux going into mitochondria, thus preventing the complete oxidation of glucose [14, 16]. Due to aerobic glycolysis, more glycolytic metabolites are shunted to pathways of production of building blocks (e.g., ribose) and reducing agents (NADPH), both of which are required for macromolecule biosynthesis in cell proliferation [17–19]. In addition, PDA cells are also highly dependent on glutamine as a nitrogen source for the biosynthesis necessary for PDA cell proliferation [20–23].

Mitochondrial uncoupling is a process that facilitates protons influx across the inner mitochondrial membrane without generating ATP [24, 25], which causes a futile TCA cycle with mitochondrial oxidation and ultimately promotes glucose and glutamine oxidation. For that reason, we postulate that mitochondrial uncoupling could potentially diminish the anabolic effect of aerobic glycolysis and exhaust glutamine, thereby inhibiting cancer cell proliferation. Small molecule mitochondrial uncouplers have been used in humans before. In the 1930s, 2,4-dinitrophenol (DNP) was a proved drug used by more than 100,000 people for weight loss in a period of 4 years [26]. However, DNP has a narrow therapeutic index, and it was withdrawn from the market. Another mitochondrial uncoupler used in humans is niclosamide, an anthelmintic drug [27]. In contrast to DNP, NEN exhibits a wide therapeutic index, partly due to its limited absorption and restricted distribution, such as enriched in the liver with limited exposure to other tissues [28]. Previously, we demonstrated that the ethanolamine salt of niclosamide, niclosamide ethanolamine (NEN), and oxyclozanide (a veterinary anthelmintic drug with mitochondrial uncoupling activity) are efficacious for treating hepatic metastasis of colorectal cancer in the murine models [29]. The similar anticancer activity was observed with a slow-release form of DNP [30].

It remains to be tested if pancreatic cancers would respond to the mitochondrial uncoupling therapeutic strategy as colon cancers [29]. Our initial in vivo efficacy testing of NEN in murine models did not produce consistent results (data not shown). NEN has multiple intrinsic limitations as a cancer drug candidate. For example, NEN contains a moiety of nitrobenzene structure, which is often mutagenic and Ames positive [31]. Moreover, the absorption of NEN is low and varies between individuals. To overcome these shortcomings, we have implemented a medicinal chemistry program to synthesize and screen new mitochondrial uncouplers with better druggable properties. One compound, MB1-47 (5-chloro-2-hydroxy-3-methyl-N-(6-(trifluoromethyl)benzo[d]thiazol-2-yl) benzamide, 2-aminoethan-1-ol salt) was identified. In this report, we examined the metabolic effect of MB1-47, and its anticancer activity in cultured pancreatic cancer cells and in murine models of PDA hepatic metastasis.

Results

MB1-47 is a mitochondrial uncoupler with favorable pharmacokinetic properties

The mechanism by which chemical uncouplers uncouple oxidative phosphorylation is illustrated in Fig. 1A [32]. In essence, a chemical uncoupler is often a lipophilic weak acid distributed in the mitochondrial inner membrane (MIM), where it exists in equilibrium between the protonated form (UH) and deprotonated form (U-). When a protonated uncoupler (UH) moves to the inner side of the MIM (matrix side), the protonated uncoupler (UH) tends to release the proton to the mitochondrial matrix and become deprotonated. The protonation–deprotonation of an uncoupler within the MIM thus catalyzes a passive translocation of protons across the MIM.

The synthesis route and chemical structure of MB1-47 are shown in (Fig. 1B) with detailed synthesis conditions described in the "Material and Method" section. The hallmark of mitochondrial uncoupling is the induction of oxygen consumption in the presence of ATP synthase inhibitor oligomycin (i.e., increasing the electron transport chain activity independent of ATP synthesis). We tested the uncoupling activity of MB1-47 with oxygen consumption rate (OCR) assay with the Seahorse XF24 instrument in murine pancreatic adenocarcinoma cells, Panc02. MB1-47 increases the OCR in the presence of oligomycin at 2.5 µM (Fig. 2A), indicating MB1-47 is a mitochondrial uncoupler. The mitochondrial uncoupling process is usually correlated with a reduction in mitochondrial membrane potential (MMP). To confirm the uncoupling effect of MB1-47, Panc02 cells were treated with various concentrations of MB1-47, and MMP was measured in these cells with the TMRE staining method. Our data show that MB1-47 begins to reduce the MMP at 0.5 µM (data not shown), reduces roughly 30–50% of staining at 1.0 µM, and nearly completely dissipates the MMP at 2.5 µM (Fig. 2B). Similar results were obtained with another pancreatic cancer cell line, Panc1 (Supplementary Fig. S1a, b). As mitochondrial uncouplers usually have high protein binding capacity, we determined the effect of MB1-47 on MMP in the medium containing no fetal bovine serum (FBS). As summarized in Fig. S1c, MB1-47 exhibits robust activity in reducing MMP at 10 nM in the medium containing no FBS, as observed with

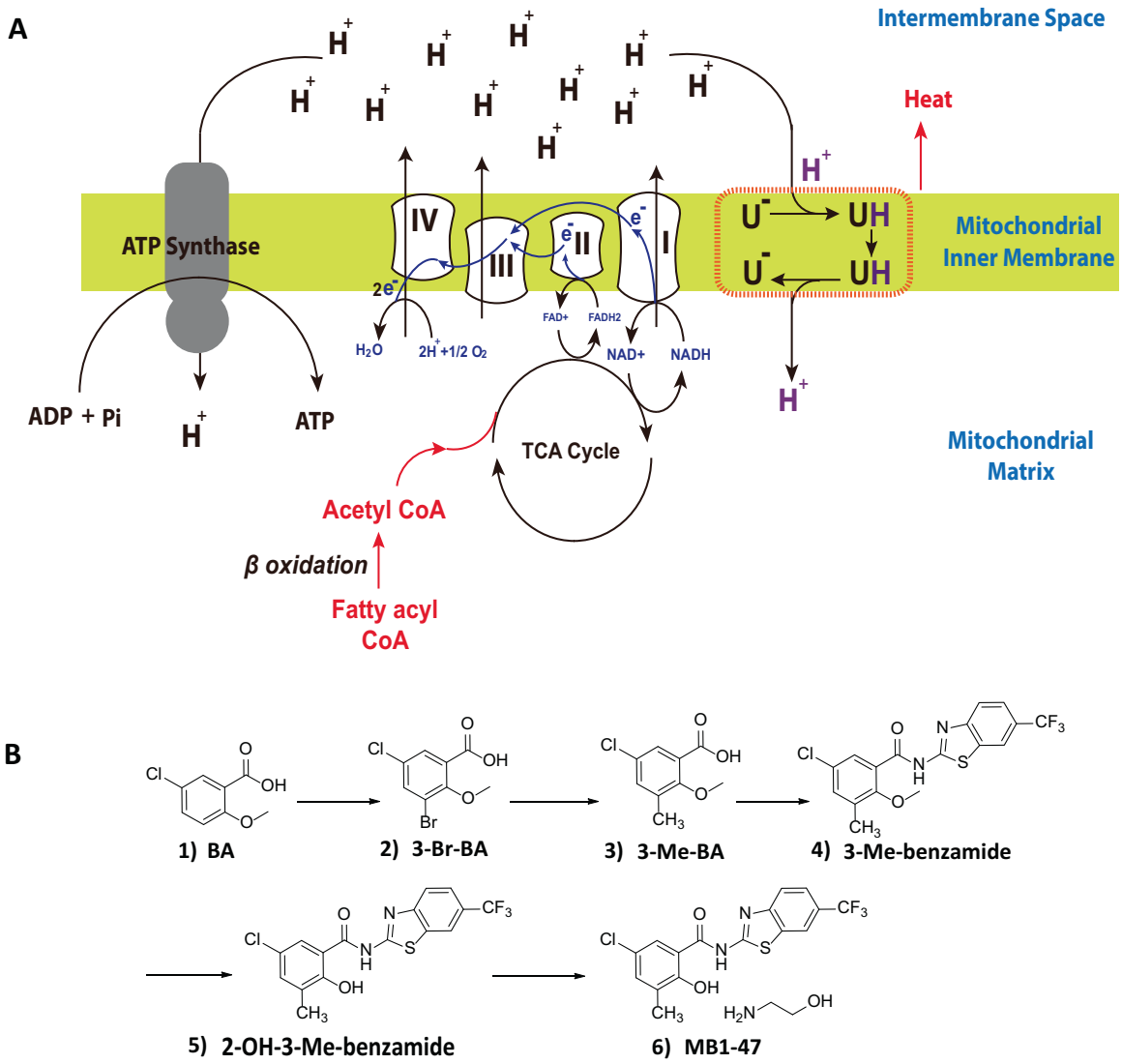

Fig. 1 The schematic of the mitochondrial uncoupling mechanism and the synthetic route of MB1-47. A Mechanistic illustration of a chemical uncoupler (UH) showing a schematic of oxidative phosphorylation and chemical uncoupling. The ETC (electron transport chain) complexes pump protons out of the mitochondrial inner membrane (MIM), resulting in a proton gradient driving ATP synthesis. A chemical uncoupler (U^-) catalyzes a protonation/deprotonation cycle that facilitates a proton influx which does not generate ATP, leading to a "futile" oxidation of acetyl-CoA. **B** The synthetic route and chemical structure for MB1-47 (detailed synthetic methods are described in "Materials and Methods"): 1 BA (5-chloro-2-methoxybenzoic acid), in sulfuric acid, TFA, and NBS to yield 2 Br-BA (3-bromo-5-chloro-2-methoxybenzoic acid). Next the reaction was acidified using HCl and extracted using ethyl acetate to eventually yield 3 3-Me-BA (5-chloro-2-methoxy-3-methylbenzoic acid). It was then further catalyzed using DMF and purified to yield 4 3-Me-benzamide (5-chloro-2-methoxy-3-methyl-N-(6-(trifluoromethyl)benzo[d]thiazol-2-yl)benzamide). 5 2-OH-3-Me-benamide (5-chloro-2-methoxy-3-methyl-N-(6-(trifluoromethyl)benzo[d]thiazol-2-yl)benzamide) was combined with pyridinium chloride to yield 6 MB1-47 (5-chloro-2-hydroxy-3-methyl-N-(6 (trifluoromethyl) benzo[d]thiazol-2-yl)benzamide).

NEN [32]. The effect of MB1-47 on OCR correlates with its effect on the MMP, for example, in a medium containing 10% FBS, the indication of OCR is observable at a concentration of 0.5 μM (data not shown), becomes robust at 1.0 μM, and reaches maximal at 2.5 μM (Fig. S1d, e).

Next, we performed pharmacokinetic studies of MB1-47. Our data show that MB1-47 has significantly improved pharmacokinetic properties over NEN, including higher exposure and prolonged half-life (Fig. 2C) [28]. Moreover, consistent with high plasma protein binding property (Fig. 2C) [28], MB1-47 has a low volume of distribution (Fig. 2C) and has enriched distribution in the liver (Fig. 2C). For further testing MB1-47 in mouse models, we titrated the dosage of MB1-47 in a chow diet and measured the blood concentration of MB1-47. We found that feeding the mice with chow containing 600 ppm MB1-47 mice exhibit a fluctuation MB1-47 between 0.5 and 1.4 μM in plasma (Fig. 2D), sufficient to induce mitochondrial uncoupling in vivo.

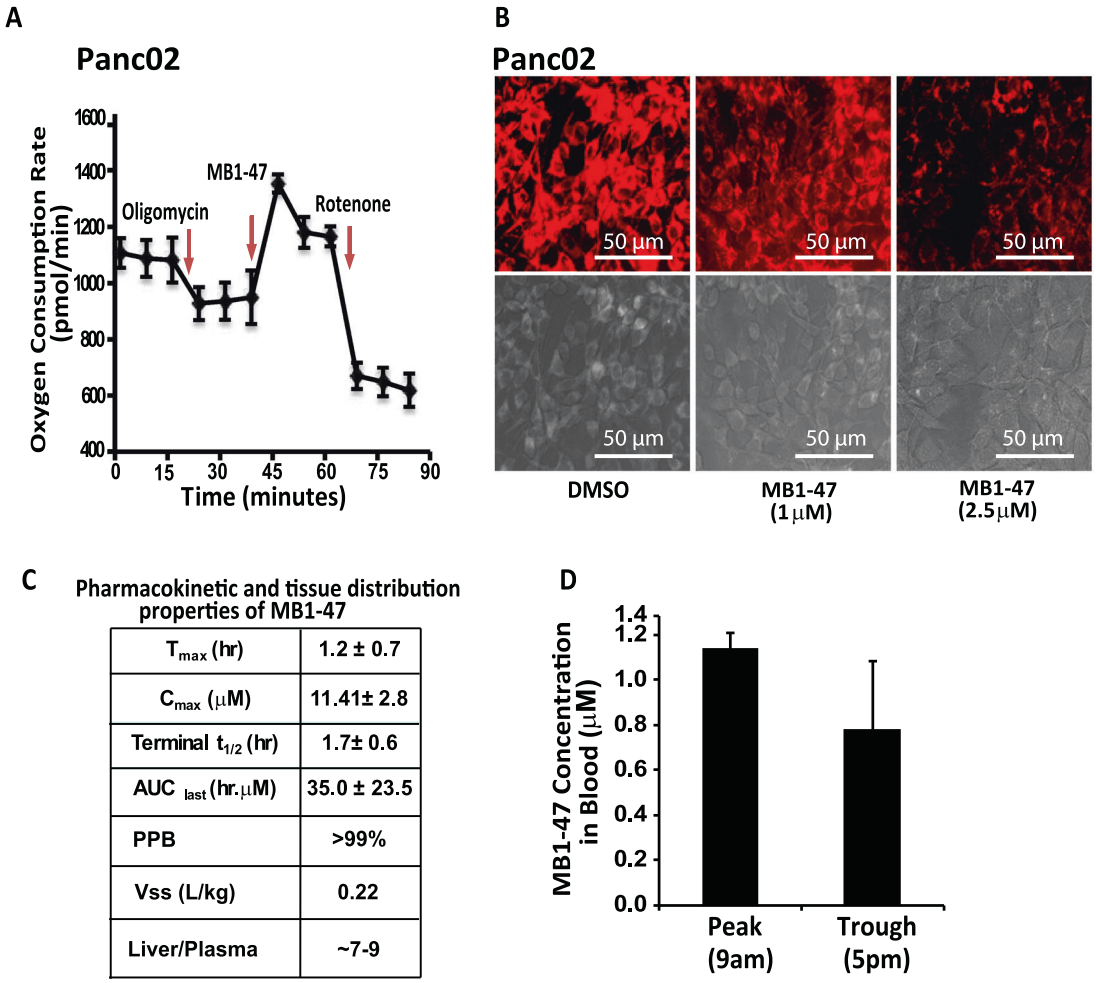

T_{max} (hr)	1.2 ± 0.7
C_{max} (µM)	11.41± 2.8
Terminal $t_{1/2}$ (hr)	1.7± 0.6
AUC $_{last}$ (hr.µM)	35.0 ± 23.5
PPB	>99%
Vss (L/kg)	0.22
Liver/Plasma	~7-9

Fig. 2 MB1-47 uncouples mitochondria in pancreatic cancer cells. **A** Oxygen consumption rate (OCR) of Panc02 cells measured by Seahorse X24. This was carried out with sequential addition of oligomycin (final concentration of 5 µM), MB1-47 (final concentration 2.5 µM), and rotenone (final concentration of 2.5 µM), at indicated time points. **B** Effective concentrations of MB1-47 for mitochondrial uncoupling in Panc02 cells measured with TMRE staining method. Panc02 cells were treated with various concentrations of MB1-47 or vehicle (DMSO) for 2 h, followed by staining with TMRE for 10 min. **C** Pharmacokinetic and tissue distribution properties of oral MB1-47 (10 mg/kg). PPB plasma protein binding, Vss volume of distribution, Liver/Plasma distribution ratio between liver (mg/g) and plasma (µg/ml). **D** Blood concentration analyses (µM) in mice measured at 9 a.m. (peak) and 5 p.m. (trough) in mice fed the diet containing MB1-47 (600 ppm) for 2 weeks. **B**, **C** are representative results from three independent experiments. **D**, **E** are representative results from two independent experiments. Results in (**B**) are indicated as means ± SD values.

The effect of MB1-47 on pancreatic cancer cell metabolism

To study the metabolic consequences of MB1-47 treatment, we incubated Panc02 cells with [U-$^{13}C_6$]-glucose, extracted and analyzed the metabolites using LC-MS approach. Our focus revolves around the metabolism of the central carbon in glycolysis and the TCA cycle (Fig. 3A), and the [U-$^{13}C_6$]-glucose allows us to measure metabolic flux rates. The cells were treated with MB1-47 at 1 µM, an intermediate concentration in the range between 0.5 and 2.5 µM that activates mitochondrial uncoupling. Consistent with increased mitochondrial oxidation rate, our LC-MS results show higher glucose to TCA cycle flux in the MB1-47-treated cells, as demonstrated by elevated levels of two-carbon ^{13}C incorporated into TCA cycle metabolites. For example, [U-$^{13}C_6$]-glucose generates $^{13}C_3$-pyruvate and $^{13}C_2$-acetyl-CoA, and in turn generates $^{13}C_2$-succinate (Fig. 3B), malate (Fig. 3C), both of which increased in the MB1-47-treated cells. Consistent with our hypothesis, as a result of futile oxidation, the pool size (the absolute level) of glutamate is decreased (Fig. 3D). In addition, the pool sizes of most amino acids (exception for methionine) either decreased significantly after 1-h treatment or exhibited a trend of decreasing (Supplementary Fig. S2).

Consistent with a futile cycle, our results showed that MB1-47 treatment increased the ratios of AMP/ATP (Fig. 3E) and ADP/ATP (Fig. 3F), as well as a decrease in UTP (Fig. 3G) and elevation of the UMP/UTP ratio (Fig. 3H).

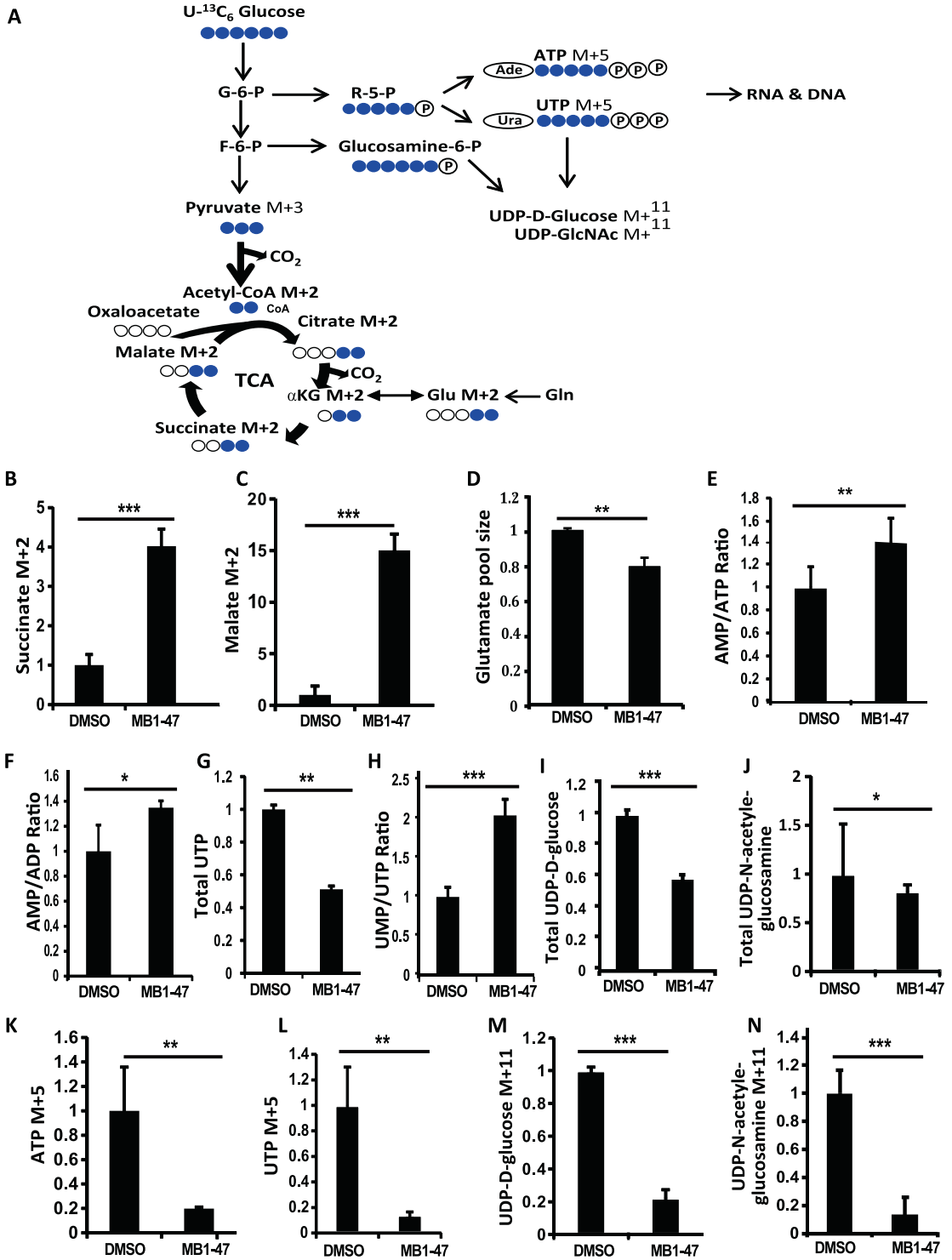

Fig. 3 Effect of MB1-47 on pancreatic cancer cell metabolism. A Schematic representation of metabolic molecules measured in the LC-MS experiments. Each oval shape represents a carbon atom of a molecule, with ^{13}C represented by an oval in blue (●), and ^{12}C by an oval in white (○). In (**B**–**N**), relative levels or ratios of metabolites, as indicated in each panel, in control (DMSO treated) Panc02 cells or cells treated with MB1-47 (1.0 μM). From **B** to **N**, Panc02 cells were grown in a medium containing 100% U-^{13}C glucose, treating with 1.0 μM MB1-47 or vehicle DMSO for 1 h. The metabolites were extracted using cold 40:40:20 methanol:acetonitrile:water w/ 0.5% formic acid (ice cold) mixture. The levels of both pooled (^{12}C and ^{13}C metabolites) and ^{13}C labeled metabolite were measured by LC/MS (Q Exactive PLUS hybrid quadrupole-orbitrap mass spectrometer (Thermo Scientific) coupled to hydrophilic interaction chromatography (HILIC)). G6P glucose-6-phosphate, F6P fructose-6-phosphate, R-5-P ribose 5-phosphate, Glu Glutamate, αKG alpha-ketoglutarate. The data are representative results from two independent experiments; each has sample treatment in triplicate. Results are showed as means ± SD values and statistical significance (*P*) was determined by Student *t* test: $*P < 0.05$; $**P < 0.01$; $***P < 0.001$.

The synthesis of sugar nucleotides is downregulated, which uses UTP as a substrate, as shown in the decreased levels of UDP-glucose (Fig. 3I) and UDP-N-acetyl glucosamine (Fig. 3J). Both nucleotide de novo synthesis and salvage use 5-phosphoribosyl-pyrophosphate as a key intermediate, which requires ATP to synthesize. After MB1-47 treatment, ATP M + 5 (Fig. 2K) and UTP M + 5 (Fig. 3L) decreased, as well as UDP-D-glucose M + 11 (Fig. 3M) and UDP-N-acetyl glucosamine M + 11 (Fig. 3N) (six from glucose and five from ribosyl); all are consistent with decreased nucleotide synthesis.

Collectively, these results demonstrate that MB1-47 accelerates pyruvate oxidation and TCA turnover, increases AMP/ATP ratio, and decreases both nucleotide and sugar production.

MB1-47 arrests cell cycle progression at G0/G1 and reduces the colony formation of pancreatic cancer cells

Next, we studied the effect of MB1-47 on murine and human pancreatic cancer cell proliferation. First, we studied the effect of MB1-47 on the cell cycle profile of pancreatic cancer cells, Panc02 and Panc1. MB1-47 inhibits cell proliferation by arresting cells in G_0/G_1 (Fig. 4A, B). The anticancer action of MB1-47 was further investigated with colony formation assay. Continuous exposure to MB1-47 led to over 90% (1.0 μM) to near 100% (2.5 μM) reduction in colony formation (Fig. 4C, D). Next, we sought to study the MB1-47 effect on the growth and proliferation of other types of pancreatic cancer cells. Seven pancreatic cell lines were treated with MB1-47 for 48 h, and cell growth and proliferation were evaluated by sulforhodamine B staining assay [33]. The results revealed that MB1-47 inhibits pancreatic cancer cell growth and proliferation in a dose-dependent manner, with IC_{50} between 0.5 and 1 μM (Fig. 4E).

MB1-47 inhibits pancreatic cancer growth in the murine models

We further tested the anticancer effect of MB1-47 in tumor transplantation mouse models. First, intrahepatic transplantation of Panc02 was performed in NSG/6 mice followed by immediate MB1-47 treatment. MB1-47-treated group exhibited a smaller tumor size compared to the control untreated group (Fig. 5A–C). Next, we tested the efficacy of MB1-47 on tumor growth after the tumor has been established, by starting MB1-47 treatment 10 days after cancer transplantation. Again, the MB1-47-treated group showed a much smaller tumor volume compared to the control untreated group (Fig. 5D–F).

MB1-47 inhibits hepatic metastasis of pancreatic cancer

Hepatic metastasis is a major cause of death in patients with pancreatic tumors, and the liver is the most common site of pancreatic cancer metastasis [8, 34]. To examine the effect of MB1-47 on the hepatic metastasis of pancreatic cancer in a well-established mouse model by injecting Panc02 cells intrasplenically into immune-deficient NSG mice (34). Two days after the recovery from the surgery, MB1-47 treatment was initiated. As shown in Fig. 6A–D, MB1-47-treated mice have less metastatic tumor nodules in the liver and smaller tumor volume compared to the control group.

Toxicology study of MB1-47

To investigate the potential toxicity effect of MB1-47 at the therapeutic dosages, a 5-day, two-dosage comprehensive toxicology study was performed in rats, the most commonly used rodent model for a preclinical toxicology study. Pharmacokinetic studies were first performed to determine the two toxicology dosages, with the goal of generating equal or higher plasma levels of the drug observed in the efficacy study (Fig. 2D), which was further confirmed by toxicokinetic results (Supplementary Results).

The toxicology data set is included in the Supplementary Results with a summary presented in Supplementary Figs. S3 and S4. As shown in Fig. S3, animal body weight continued to grow in the treated period, food intake was slightly higher in the high dosage group comparing to the low dosage group (consistent with the mechanism of action of the drug), and no elevation in body temperature (a major concern of the mechanism) was observed. Moreover, no clinical adverse effects were observed and no mortality occurred in the treatment period (Supplementary Results).

As shown in Fig. S4, hematology did not show clinical toxicology signs; however, statistically significant changes were observed, including neutrophil and monocytes counts, red blood cell size distribution (RDW-CV or RDW-SD), and mean corpuscular hemoglobin concentration, platelet distribution width, suggesting that MB1-47 affects hematogenesis. The serum chemistry showed no sign of liver toxicity. Moreover, beneficial decreases in plasma total cholesterol and AST levels were observed in the high dosage group. A significant increase in creatine levels was observed in the high dosage group. The elevated creatine levels are still in normal range, suggesting mild impact in kidney function.

MB1-47 induces AMPK activation and downregulates mTOR in the pancreatic cancer

AMPK is the master regulator for cell energy hemostasis and plays a crucial role in cell metabolism [35]. A high AMP/ATP

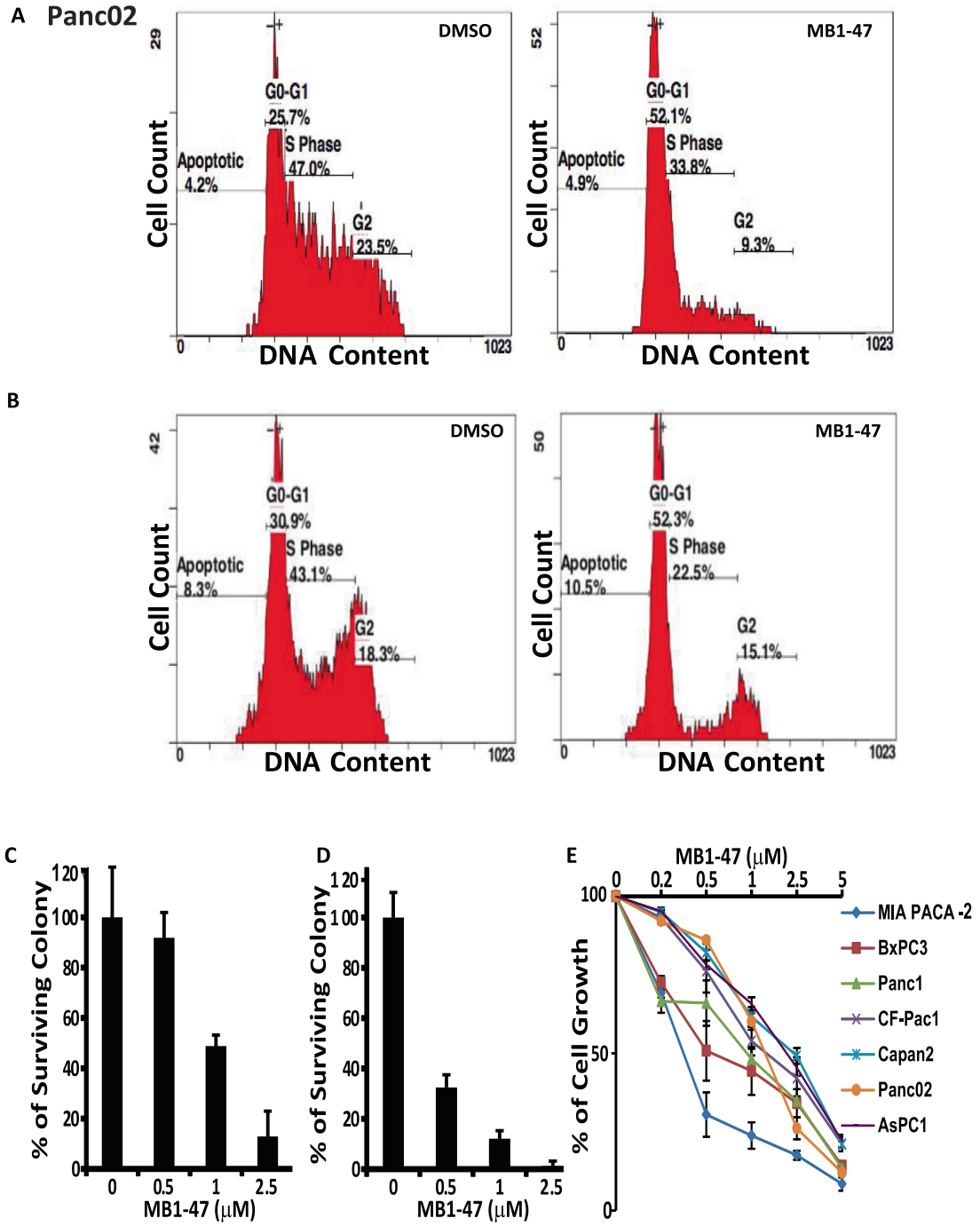

Fig. 4 Effect of MB1-47 on cell cycle progression, clonogenicity, and cell proliferation of pancreatic cancer cells. In (**A**, **B**), the flow cytometry analysis charts have the *Y*-axis as the cell count correlated with the fluorescence intensity, while the *X*-axis represents the DNA content stained with the propidium iodide dye. MB1-47 arrests pancreatic cancer cells at the G_0–G_1 phase for both Panc02 (**A**), Panc1 (**B**) cells that were treated either with vehicle (DMSO) (left panel) or 2.5 μM of MB1-47 (right panel) for 48 h, followed by cell cycle progression analysis via flow cytometry. **C**, **D** are bar graphs representing results of clonogenicity assay with % of surviving colony indicated by the *Y*-axis, while MB1-47 concentrations, 0, 0.5, 1, and 2.5 μM, are indicated by the *X*-axis. MB1-47 reduces the clonogenicity of pancreatic cancer cells Panc02 (**C**) and Panc1 (**D**), respectively. **E** MB1-47 inhibits the growth of eight pancreatic cancer cell lines: MIA PACA-2, BxPC3, Panc1, CF-Pac1, Capan2, Pan02, and AsPC1. Pancreatic cancer cells were treated with various concentrations of MB1-47: 0, 0.2, 0.5, 1, 2.5, or 5 μM for 48 h (*X*-axis), and cell growth was measured and quantified using the sulforhodamine B (SRB) staining (described in the "Materials and Methods") and calculated in % of cell growth normalized using MB1-47 treated against untreated samples (*Y*-axis). The data shown in (**A**–**E**) are representative results from three independent experiments. Results from (**C**–**E**) are shown as means ± SD. Statistical significance (*P*) between the control and treated cells was determined by Student *t* test: ***, $P < 0.001$.

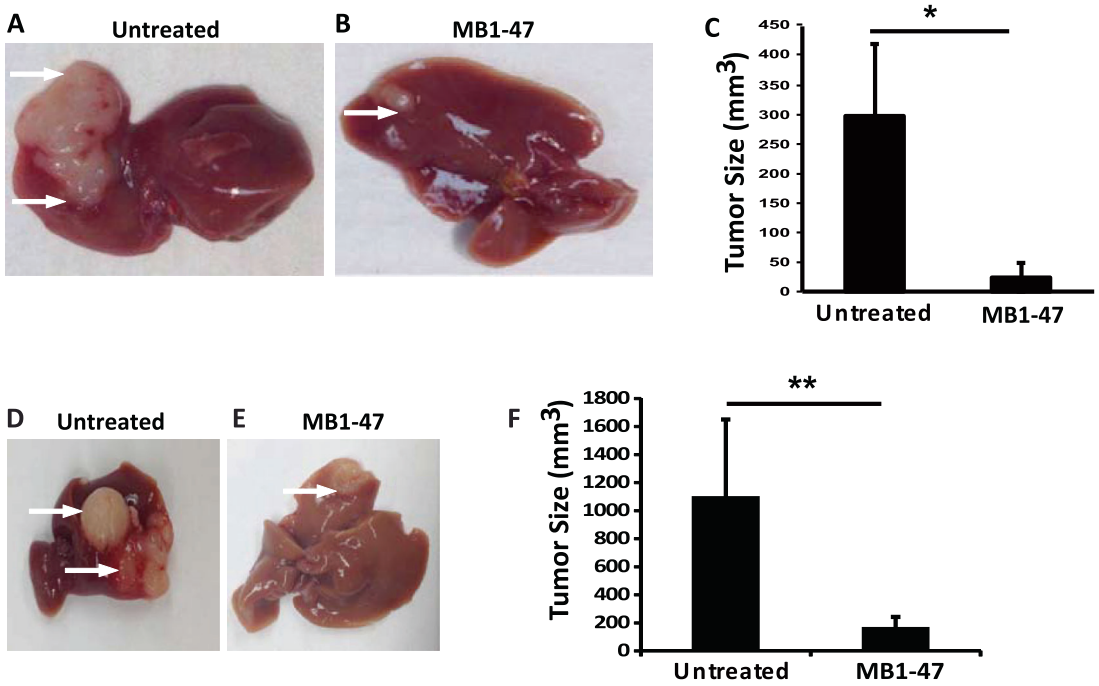

Fig. 5 MB1-47 inhibits the growth of intrahepatically transplanted Panc02 cancer cells. Showing the tumors from the mouse liver after intrahepatic injection of Panc02 cells into male NSG mice, in the absence (**A**) or presence (**B**) of 750 ppm MB1-47 diets for 3 weeks. Arrows in each picture are pointing to the presence of tumors. **C** A bar graph showing quantification of liver tumor in size (mm^3). The representative pictures of mouse liver samples from mice after intrahepatic injection of Panc02 cells to the NSG mice, fed with normal diet for 1 week (for mouse tumor to establish), then fed the normal diet (**D**) or the diet containing 750 ppm MB1-47 (**E**) for 2 additional weeks. Arrows point to the locations of tumors. In (**F**), quantification of liver tumor size (mm^3) in the mice with or without 750 ppm of MB1-47 treatment as indicated. Data are shown in (**C**, **F**) as means ± SD. Statistical significance (*P*) was determined by Student *t* test between the control and MB1-47 fed mice. $N = 6$ in each group. $^*P < 0.05$. The data are representative results from two independent experiments.

ratio activates AMPK, which, in turn, can inhibit the anabolic signaling pathways and stimulate the catabolic signaling pathways [36]. In light of the effect of MB1-47 on increasing AMP/ATP ratio, we tested AMPK activity in Panc02 and Panc1 cells upon treatment with MB1-47, to confirm this signaling event. Additionally, we studied the effect of MB1-47 on AMPK's key downstream effectors, including ACC (acetyl-CoA carboxylase), the key regulator of lipid metabolism whose activity promotes lipid synthesis and inhibits lipid oxidation at the same time, mTOR [37], the key regulator for protein synthesis, as well as ERK, which is involved in a pro-proliferation pathway important for PDA cells.

Our results indicated that MB1-47 activates AMPK in a dose-dependent manner at concentrations that induce mitochondrial uncoupling (Fig. 7A–C, with quantification in Fig. S5). Moreover, MB1-47 led to an increase in ACC phosphorylation, which is expected to diminish ACC activity, and consequently inhibiting lipid synthesis and promoting lipid oxidation (Figs. 7A–C and S5). As shown in (Figs. 7D–E and S5), MB1-47 treatment decreases the phosphorylation of P70S6K and 4E-BP1, indicative of the downregulation of mTOR activity. The results also showed that MB1-47 decreases the activity of ERK1/2 signaling pathways in cancer pancreatic cancer cells (Figs. 7D–E and S5).

Discussion

In this study, we explored the strategy of treating PDA by changing cell metabolism. Using both in vitro and in vivo models, we demonstrated that a mitochondrial uncoupler, MB1-47, inhibits cancer cell growth and proliferation, decreases clonogenic activity, inhibits both tumor growth in vivo and metastasis to the liver in mice.

Mitochondrial uncoupling leads to a futile cycle that accelerates the rate of mitochondrial oxidation (Fig. 1A). The anticancer mechanism is proposed in the working shown in Fig. 7F. Primarily, the futile oxidation diminishes the metabolites feeding into pathways for the production of building blocks and NADPH required for the biosynthesis of macromolecules such as nucleic acids, lipids, and proteins. In parallel, the reduction of ATP synthesis activates nutrient deprivation signal pathways mediated by AMPK, leading to inhibition of ACC, mTOR, and ERK pathways. It is possible that these energetic, biomaterial, and signaling events reinforce each other, effectively shut down cell growth and proliferation programs.

Previously, we demonstrated that mitochondrial uncouplers NEN and oxyclozanide are efficacious for treating hepatic metastasis of colorectal cancer in murine models [29]. When

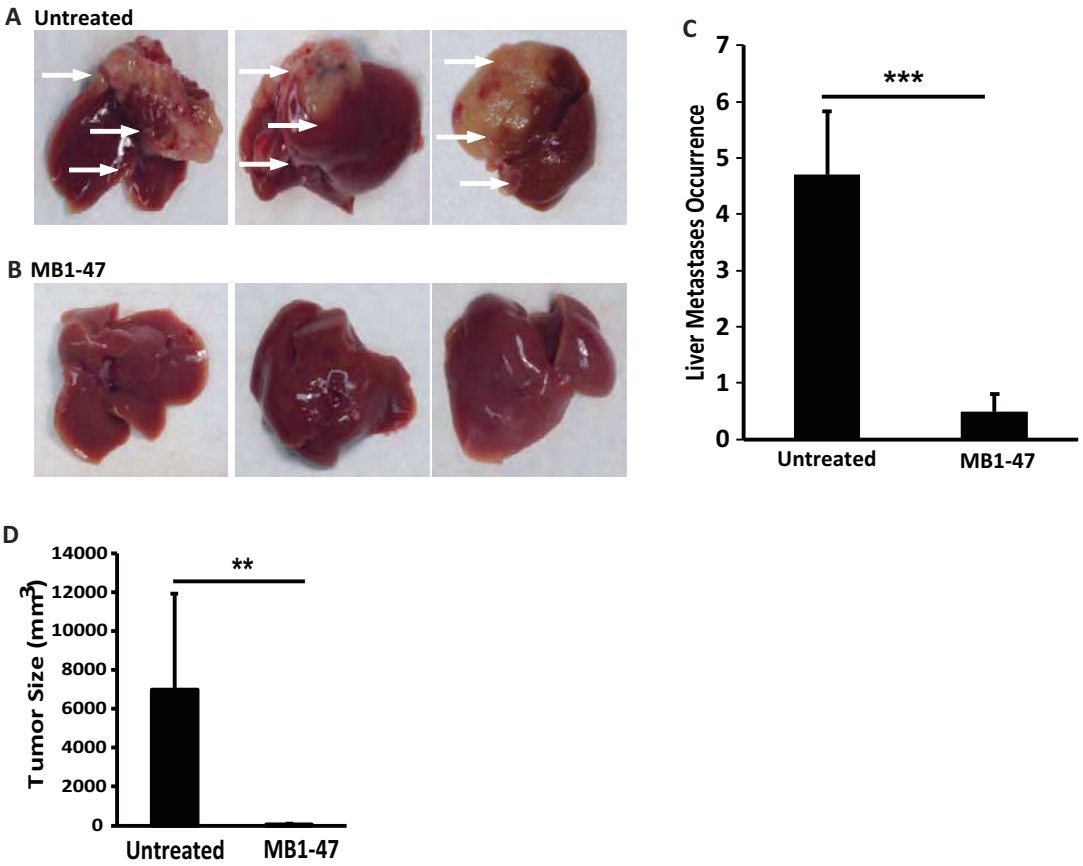

Fig. 6 MB1-47 inhibits liver metastasis of the intrasplenically injected Panc02 cells. Representative pictures of the liver from the NSG mice after intrasplenic injection of Panc02 cells, either fed with normal chow diet (**A**) or with the diet containing 750 ppm MB1-47 (**B**) for 2 weeks. Arrows pointing to the tumor nodules. The quantification of visible hepatic tumor nodules resulted from metastasis with or without MB1-47 treatment is as described in the Experimental Methods and plotted in (**C**) as a bar chart. The *Y*-axis represents the liver metastasis occurrence, while the *X*-axis describes the type of diet, untreated versus 750 ppm MB1-47. **D** Quantification of the average tumor size measured on the mice with liver metastasis, untreated versus 750 ppm MB1-47. Data are shown as means ± SD. Statistical significance (*P*) was determined by Student *t* test between the control and MB1-47 fed mice. $N = 7$ in each group. $^{**}P < 0.01$ and $^{***}P < 0.001$. The data are representative results from two independent experiments.

testing the efficacy of NEN in treating pancreatic cancer in animal models, we failed to obtain consistent and robust results (data not shown). We suspected that the lack of consistent efficacy is due to low systemic exposure as results of poor absorption and poor target organ distribution. For that reason, MB1-47 was designed and screened for retaining the mitochondrial uncoupling potency with liver-enriched distribution as NEN, meanwhile overcoming some unfavorable features. MB1-47 has a higher absorption after oral administration, a higher systemic exposure, and absence of the oncogenic potential (Ames test negative). With those improved properties, in this study, we showed that MB1-47 exhibits robust anticancer activity in vivo in pancreatic cancer animal models, both inhibiting growth of the transplanted tumor as well as inhibiting the hepatic metastasis.

In addition to efficacy, potential toxicity is one of the main hurdles for therapeutics development. Our preliminary toxicology showed that at therapeutically relevant levels, MB1-47 does not seem to cause overt toxicity as examined by body weight increase, food consumption, body temperature, clinical observation, hematology, serum chemistry, and histology analysis. It is particularly encouraging that no impact on body temperature and no drug accumulation were observed, as those issues were previously associated with the toxicology presentation of DNP in humans. However, the study did show that MB1-47 may mildly affect hematogenesis and kidney function. Long-term toxicology studies with escalating dosages are warranted to further address the potential toxicity issues.

In conclusion, we demonstrated that a new mitochondrial uncoupler, MB1-47, has anticancer activity in vitro and is efficacious against hepatic metastatic PDA in murine models. The results support that the anticancer mechanism is related to the alteration of cancer cell metabolism. The unique mechanism of targeting mitochondria and cancer cell metabolism may provide a new therapeutic strategy for PDA, the deadly cancer essentially refractory to all current therapeutic approaches. While further research is necessary, in particular

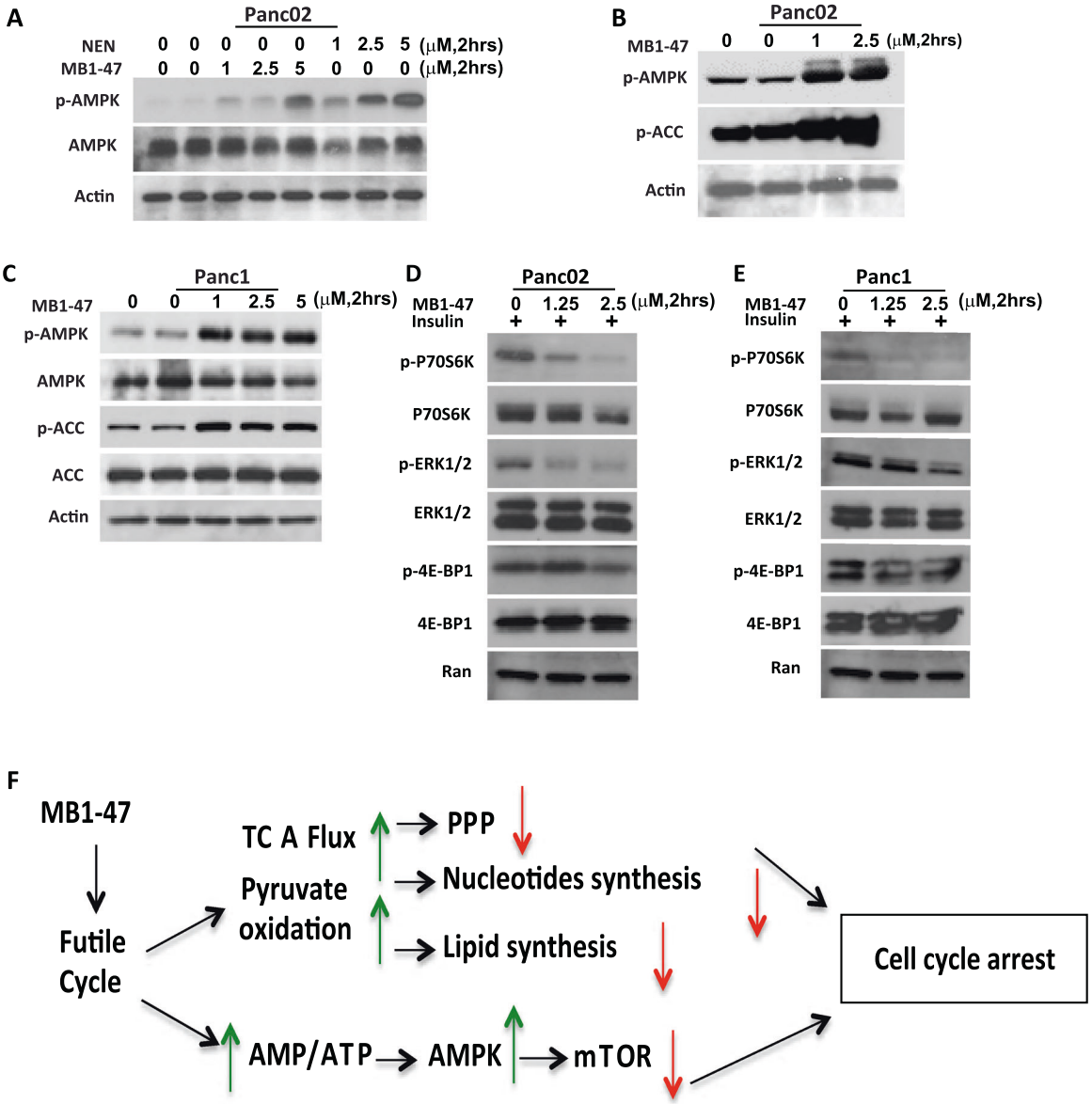

Fig. 7 MB1-47 increases phosphorylation of AMPK and ACC and downregulates mTOR activities in the pancreatic cancer cells. A Immunoblot analyses showing that NEN and MB1-47 increase phosphorylation of AMPK in Panc02 cells. Immunoblot analyses showing that MB1-47 increases phosphorylation of AMPK and ACC in Panc02 (**B**) and Panc1 cells (**C**), respectively. Immunoblot analyses of Panc02 (**D**) and Panc1 (**E**) cells, respectively, showing that MB1-47 reduces the mTOR activity and ERK phosphorylation levels under insulin stimulation. **F** The working model on the anticancer mechanism of action of MB1-47. Immunoblotting analyses (**A**–**E**) are representative results from three independent experiments. Quantification of the immunoblotting analyses is shown in Supplementary Fig. S5.

in toxicology, MB1-47 represents a promising prototype for the therapeutic strategy.

Materials and methods

All materials and methods are in the supplementary file.

Acknowledgements The authors want to thank Frank Leu for reviewing and editing the paper. The project was partially funded by Rutgers Busch Biomedical Award (2014), HCED Iraq Scholarship program, New Jersey Cancer Commission Research (NJCCR) Fellowship, and Mito BioPharma, LLC. AA is supported by HCED Iraq Scholarship program. HT was supported in part by NJCCR. AA, HT, JG, and SJ are partially supported by NIH (1R21CA216604 and 1R21 AA027050).

Author contributions Conception and design: SJ and AA. Development of methodology: AA, SJ, BC, and DA. Acquisition of data: BC synthesized the compound, AA conducted most of the biological experiments, AA and HT conducted OCR Seahorse experiment, AA, JG, and XS conducted the LC-MS experiment. Analysis and interpretation of data (e.g., statistical analysis, LC-MS): AA, XS, and SJ. Writing, review, and/or revision of the paper: AA and SJ. Study supervision: SJ.

Compliance with ethical standards

Conflict of interest SJ is a founder of Mito BioPharma, which has a license right from Rutgers University for developing safe mitochondrial uncouplers for treating cancer and metabolic diseases. BC, HT, and DA are co-inventors of the patents covering the rights of MB1-47 and its derivatives. The rest of the authors declare no competing interests.

Publisher's note Springer Nature remains neutral with regard to jurisdictional claims in published maps and institutional affiliations.

References

1. Siegel R, Naishadham D, Jemal A. Cancer statistics, 2015. CA Cancer J Clin. 2015;65:5–29.
2. Rahib L, Smith BD, Aizenberg R, Rosenzweig AB, Fleshman JM, Matrisian LM. Projecting cancer incidence and deaths to 2030: the unexpected burden of thyroid, liver, and pancreas cancers in the United States. Cancer Res. 2014;74:2913–21.
3. Mimeault M, Brand RE, Sasson AA, Batra SK. Recent advances on the molecular mechanisms involved in pancreatic cancer progression and therapies. Pancreas. 2005;31:301–16.
4. Stathis A, Moore MJ. Advanced pancreatic carcinoma: current treatment and future challenges. Nat Rev Clin Oncol. 2010;7:163–72.
5. Gillen S, Schuster T, Meyer zum Büschenfelde C, Friess H, Kleeff J. Preoperative/neoadjuvant therapy in pancreatic cancer: a systematic review and meta-analysis of response and resection percentages. PLOS Med. 2010;7:e1000267.
6. Conroy T, Desseigne F, Ychou M, Bouché O, Guimbaud R, Bécouarn Y, et al. FOLFIRINOX versus gemcitabine for metastatic pancreatic cancer. N Engl J Med. 2011;364:1817–25.
7. Hidalgo M. Pancreatic cancer. N Engl J Med. 2010;362:1605–17.
8. Maitra A, Hruban RH. Pancreatic cancer. Annu Rev Pathol. 2008;3:157–88.
9. Efthimiou E, Crnogorac-Jurcevic T, Lemoine NR. Pancreatic cancer genetics. Pancreatology. 2001;1:571–5.
10. Jones S, Zhang X, Parsons DW, Lin JC, Leary RJ, Angenendt P, et al. Core signaling pathways in human pancreatic cancers revealed by global genomic analyses. Science. 2008;321:1801–6.
11. Zhou W, Capello M, Fredolini C, Racanicchi L, Piemonti L, Liotta LA, et al. Proteomic analysis reveals Warburg effect and anomalous metabolism of glutamine in pancreatic cancer cells. J Proteome Res. 2012;11:554–63.
12. Hanahan D, Weinberg RA. Hallmarks of cancer: the next generation. Cell. 2011;144:646–74.
13. Blum R, Kloog Y. Metabolism addiction in pancreatic cancer. Cell Death Dis. 2014;5:e1065.
14. Vander Heiden MG, Cantley LC, Thompson CB. Understanding the Warburg effect: the metabolic requirements of cell proliferation. Science. 2009;324:1029–33.
15. DeBerardinis RJ, Lum JJ, Hatzivassiliou G, Thompson CB. The biology of cancer: metabolic reprogramming fuels cell growth and proliferation. Cell Metab. 2008;7:11–20.
16. Faubert B, Boily G, Izreig S, Griss T, Samborska B, Dong Z, et al. AMPK is a negative regulator of the Warburg effect and suppresses tumor growth in vivo. Cell Metab. 2013;17:113–24.
17. Lunt SY, Vander Heiden MG. Aerobic glycolysis: meeting the metabolic requirements of cell proliferation. Annu Rev Cell Dev Biol. 2011;27:441–64.
18. Levine B. Cell biology: autophagy and cancer. Nature. 2007;446:745–7.
19. Levine AJ, Puzio-Kuter AM. The control of the metabolic switch in cancers by oncogenes and tumor suppressor genes. Science. 2010;330:1340–4.
20. Wise DR, DeBerardinis RJ, Mancuso A, Sayed N, Zhang XY, Pfeiffer HK, et al. Myc regulates a transcriptional program that stimulates mitochondrial glutaminolysis and leads to glutamine addiction. Proc Natl Acad Sci USA. 2008;105:18782–7.
21. Livingstone LR, White A, Sprouse J, Livanos E, Jacks T, Tlsty TD. Altered cell cycle arrest and gene amplification potential accompany loss of wild-type p53. Cell. 1992;70:923–35.
22. DeBerardinis RJ, Mancuso A, Daikhin E, Nissim I, Yudkoff M, Wehrli S, et al. Beyond aerobic glycolysis: transformed cells can engage in glutamine metabolism that exceeds the requirement for protein and nucleotide synthesis. Proc Natl Acad Sci. 2007;104:19345–50.
23. Son J, Lyssiotis CA, Ying H, Wang X, Hua S, Ligorio M, et al. Glutamine supports pancreatic cancer growth through a KRAS-regulated metabolic pathway. Nature. 2013;496:101–5.
24. Jastroch M, Divakaruni AS, Mookerjee S, Treberg JR, Brand MD. Mitochondrial proton and electron leaks. Essays Biochem. 2010;47:53–67.
25. Harper J, Dickinson K, Brand M. Mitochondrial uncoupling as a target for drug development for the treatment of obesity. Obes Rev. 2001;2:255–65.
26. Parascandola J. Dinitrophenol and bioenergetics: an historical perspective. Mol Cell Biochem. 1974;5:69–77.
27. Frayha GJ, Smyth JD, Gobert JG, Savel J. The mechanisms of action of antiprotozoal and anthelmintic drugs in man. Gen Pharm. 1997;28:273–99.
28. Tao H, Zhang Y, Zeng X, Shulman GI, Jin S. Niclosamide ethanolamine-induced mild mitochondrial uncoupling improves diabetic symptoms in mice. Nat Med. 2014;20:1263–9.
29. Alasadi A, Chen M, Swapna GVT, Tao H, Guo J, Collantes J, et al. Effect of mitochondrial uncouplers niclosamide ethanolamine (NEN) and oxyclozanide on hepatic metastasis of colon cancer. Cell Death Dis. 2018;9:215.
30. Wang Y, Nasiri AR, Damsky WE, Perry CJ, Zhang XM, Rabin-Court A, et al. Uncoupling hepatic oxidative phosphorylation reduces tumor growth in two murine models of colon cancer. Cell Rep. 2018;24:47–55.
31. Shimizu M, Yano E. Mutagenicity of mono-nitrobenzene derivatives in the Ames test and rec assay. Mutat Res. 1986;170:11–22.
32. Terada H. Uncouplers of oxidative phosphorylation. Environ Health Perspect. 1990;87:213–8.
33. Sun S-Y, Yue P, Dawson MI, Shroot B, Michel S, Lamph WW, et al. Differential effects of synthetic nuclear retinoid receptor-selective retinoids on the growth of human non-small cell lung carcinoma cells. Cancer Res. 1997;57:4931–9.
34. Li D, Xie K, Wolff R, Abbruzzese JL. Pancreatic cancer. Lancet. 2004;363:1049–57.
35. Wang W, Guan KL. AMP-activated protein kinase and cancer. Acta Physiol. 2009;196:55–63.
36. Fryer LG, Parbu-Patel A, Carling D. The anti-diabetic drugs rosiglitazone and metformin stimulate AMP-activated protein kinase through distinct signaling pathways. J Biol Chem. 2002;277:25226–32.
37. Xu J, Ji J, Yan X-H. Cross-talk between AMPK and mTOR in regulating energy balance. Crit Rev Food Sci Nutr. 2012;52:373–81.